

GROUND DATA PROCESSING & PRODUCTION OF THE LEVEL 1 HIGH RESOLUTION MAPS



Philippe Rossello

May 2007

CONTENTS

1. Introduction	2
2. Available data	2
2.1. SPOT image	2
2.2. LAI2000 measurements.....	3
2.3. Sampling strategy	4
2.3.1. Principles.....	4
2.3.2. Evaluation based on NDVI values	5
2.3.3. Evaluation based on classification	6
2.3.4. Using convex hulls.....	8
3. Determination of the transfer function for the two biophysical variables: LAI, fCover.....	8
3.1. The transfer function considered.....	8
3.2. Results	9
3.2.1. Choice of the method	9
3.2.2. Choice of the band combination.....	9
3.3. Applying the transfer function to the Järvelja SPOT image extraction.....	12
4. Conclusion.....	12
5. Acknowledgements	13
ANNEX.....	14



1. Introduction

This report describes the production of the high resolution, level 1, biophysical variable maps for the Järvelja site in June 2005 (see campaign report for more details about the site and the ground measurement campaign: annex or <http://www.avignon.inra.fr/valeri>). Level 1 map corresponds to the map derived from the determination of a transfer function between reflectance values of the SPOT image acquired during (or around) the ground campaign and biophysical variable measurements (LAI2000 in this case).

The derived biophysical variable maps are:

- Leaf Area Index (LAI): LAI corresponds to effective LAI derived from the description of the gap fraction as a function of the view zenith angle;
- cover fraction (fCover): it is the percentage of soil covered by vegetation between 0° and 7° view zenith angle.

The site is “mostly covered by a sub-boreal mixed forest of different age, including both conifers (Scots pine and Norway spruce) and deciduous (birch, aspen, alder). Agricultural fields are almost missing, however, a few unmanaged open areas are found”. Note that the site is quite flat (for more information, see annex or campaign report: <http://www.avignon.inra.fr/valeri>).

The site coordinates are described in Table 1:

	Lambert-Est-92 WGS-84 (units=meters)		Geographic Lat/Lon WGS-84		UTM 35, North, WGS-84 (units=meters)	
	Easting	Northing	Lat	Lon	Easting	Northing
Upper left corner	689150.0000	6468750.0000	58.31839287	27.22883161	513405.7675	6464181.4799
Lower right corner	693030.8821	6464710.9082	58.28047797	27.29159308	517100.8231	6459974.3314
Center	691090.0000	6466729.9998	58.29943541	27.26022130	515252.8387	6462077.4728

Table 1. Description of the site coordinates: they correspond to SPOT image coordinates.

The ground measurements were carried out from 28th June 2005 to 1st July 2005, while the high spatial resolution image (SPOT2, HRV1, resolution: 20 m) was acquired on 20th June 2005.

2. Available data

2.1. SPOT image

The SPOT image was acquired the 20th June 2005 by HRV1 on SPOT2. The radiometric and geometric correction was performed by SPOT image (product 1B). The image was geo-referenced by TARTU Observatory. The projection is Lambert-Est-92 (Lambert Conformal Conic 2 parallel), WGS-84. Please, refer to the campaign report for more details: annex or <http://www.avignon.inra.fr/valeri>. No atmospheric correction was applied to the image. However, as the SPOT image is used to compute empirical relationships between reflectance and biophysical variable, we can assume that the effect of the atmosphere is the same over the whole 4 x 4 km site. Therefore, it will be taken into account everywhere in the same way.

Figure 1 shows the relationship between Red and near infrared (NIR) SPOT channels: the soil line is marked and no saturated point is observed.

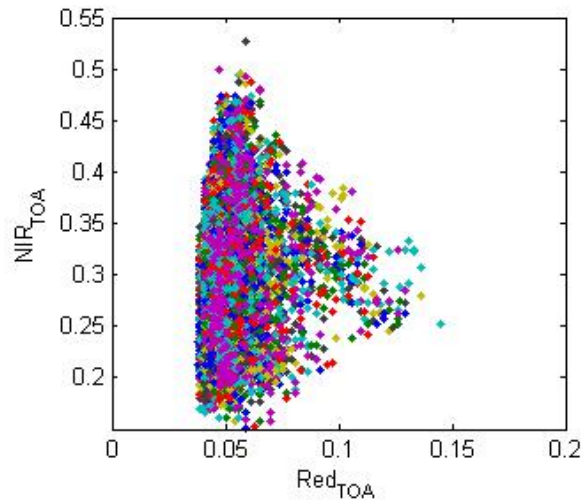


Figure 1. Red/NIR relationship on the SPOT image for Järvselja, 2005

2.2. LAI2000 measurements

For each Elementary Sampling Unit (ESU), the biophysical variables (LAI, fCover) were derived from LAI2000 instrument. The measurements have been acquired at two heights: ground level and breast height (1.30m). The two levels allow the distinction between understorey and trees. According to the sampling protocol, 48 measurements were taken at the both level for each ESU. In the VALERI context, we are interested in the whole leaf area index, therefore, the ESU biophysical variables that are used in the following were computed as:

- $LAI = LAI_{canopy} + LAI_{ground}$
- fCover is the percentage of soil covered by vegetation at 7° view zenith angle (ground level).

A comparison of processing results from LAI2000 instrument and Can-Eye software (Figure 2) developed at INRA-CSE shows that the relationship is consistent (level: LAI_canopy), even if it is more noisy for the high LAI values.

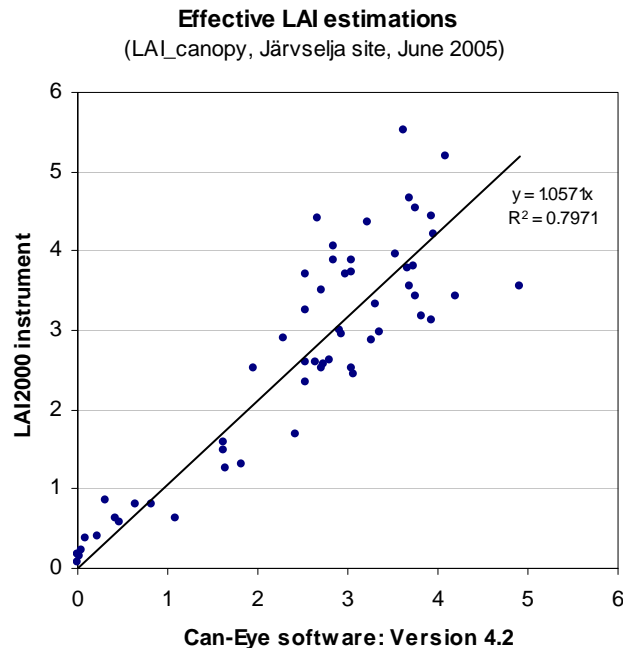


Figure 2. Comparison of processing results from LAI2000 instrument and Can-Eye software (points in blue correspond to 57 ESUs).

Figure 3 shows the distribution of the different measured variables over the sampled ESUs. LAI varies from 0.72 to 6.22 and fCover from 0.23 to 0.98. This range shows a heterogeneous site in terms of LAI with very high biophysical variable values. To build the relationships between biophysical variables and SPOT data, the



reflectance of a given forest ESU for which the height of the trees is equal or higher than 12 meters was considered as the average reflectance over the central pixel + the 8 surrounding pixels. Consequently, the fish-eye observes an area of at least $\pi \times [12 \times \tan(68^\circ)]^2 \cong 2800 \text{ m}^2$, *i.e.* close to the area of 9 SPOT pixels ($=3600\text{m}^2$) when using a maximum view zenith angle of 68° .

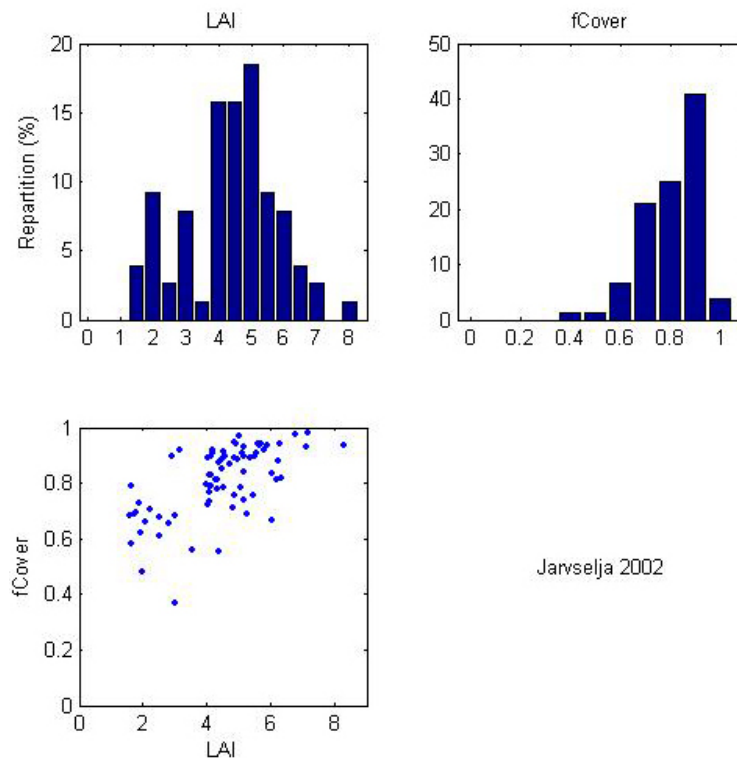


Figure 3. Distribution of the measured biophysical variables over the ESUs.

2.3. Sampling strategy

2.3.1. Principles

The sampling strategy is defined in the campaign report: <http://www.avignon.inra.fr/valeri>. It was attempting to represent as much as possible the range of variation of canopy types and conditions. In addition, some ESUs were organised within a cross pattern at the centre of the site to be able to get geostatistic estimates.

Figure 4 shows that the 57 ESUs are evenly distributed over the site (4 x 4 km). The processing of the ground data has shown that: considering that SPOT geo-location and GPS measurements are associated to errors, we found that processed LAI for E16503 did not correspond to the SPOT pixel in terms of reflectance as compared to the knowledge of the land use: it has been shifted by 1 pixel.

Finally, 57 ESUs have been kept for the computation of the transfer function:

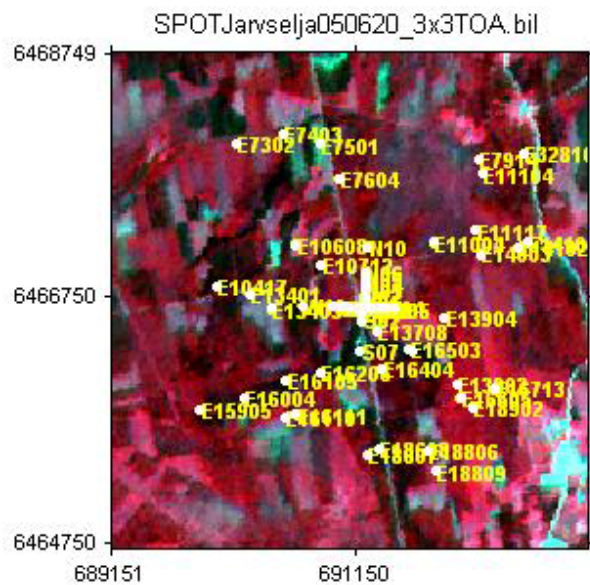


Figure 4. Distribution of the ESUs around the Järvselja site.

2.3.2. Evaluation based on NDVI values

The sampling strategy is evaluated using the SPOT image by comparing the NDVI distribution over the site with the NDVI distribution over the ESUs (Figure 5). As the number of pixels is drastically different for the ESU and whole site ($WS = 40000$ in case of a 4×4 km image at 20 m resolution), it is not statistically consistent to directly compare the two NDVI histograms. Therefore, the proposed technique consists in comparing the NDVI cumulative frequency of the two distributions by a Monte-Carlo procedure which aims at comparing the actual frequency to randomly shifted sampling patterns. It consists in:

1. computing the cumulative frequency of the N pixel NDVI that correspond to the exact ESU locations;
2. then, applying a unique random translation to the sampling design (modulo the size of the image);
3. computing the cumulative frequency of NDVI on the randomly shifted sampling design;
4. repeating steps 2 and 3, 199 times with 199 different random translation vectors.

This provides a total population of $N = 199 + 1$ (actual) cumulative frequency on which a statistical test at acceptance probability $1 - \alpha = 95\%$ is applied: for a given NDVI level, if the actual ESU density function is between two limits defined by the $N\alpha/2 = 5$ highest and lowest values of the 200 cumulative frequencies, the hypothesis assuming that WS and ESU NDVI distributions are equivalent is accepted, otherwise it is rejected.

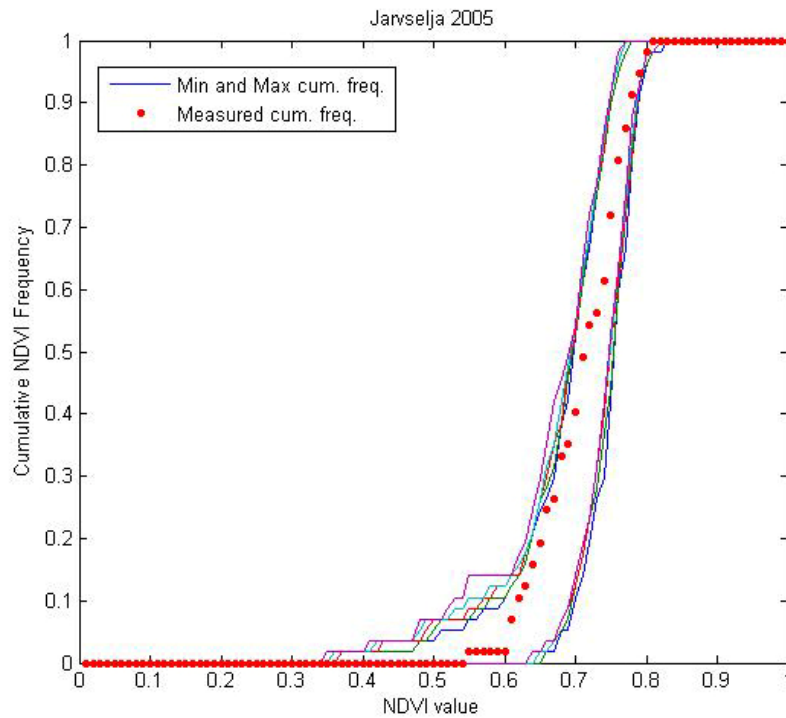


Figure 5. Comparison of the ESU NDVI distribution and the NDVI distribution over the whole image.

Figure 5 shows that the NDVI distribution of the 57 ESUs is very good over the whole site even if the cumulative frequency curve is close to the boundaries for high NDVI values comprised between 0.77 and 0.81. Note that NDVIs lower than 0.54 have not been sampled although they are present in the image. They may correspond to recent clear cuts, open areas, paths...

2.3.3. Evaluation based on classification

A non supervised classification based on the *k*_means method (Matlab statistics toolbox) was applied to the reflectance of the SPOT image to distinguish if different behaviours on the image for the biophysical variable-reflectance relationship exist.

A number of 5 classes was chosen (Figure 6). The distribution of the classes on the image and on the ESUs is mainly different at level of the classes 1 and 3. The classes 1, 2 and 5 are under-represented, while the classes 3 and 4 appear to be over-sampled.



2.3.4. Using convex hulls

A test based on the convex hulls was also carried out to characterize the representativeness of ESUs. Whereas the evaluation based on NDVI values uses two bands (red and NIR), this test uses the 3 bands (green, red and NIR in this case) of the SPOT image. A flag image, is computing over the reflectances (Figure 8). The result on convex-hulls can be interpreted as:

- pixels inside the 'strict convex-hull': a convex-hull is computed using all the SPOT reflectance corresponding to the ESUs belonging to the class. These pixels are well represented by the ground sampling and therefore, when applying a transfer function the degree of confidence in the results will be quite high, since the transfer function will be used as an interpolator;
- pixels inside the 'large convex-hull': a convex-hull is computed using all the reflectance combination ($\pm 5\%$ in relative value) corresponding to the ESUs. For these pixels, the degree of confidence in the obtained results will be quite good, since the transfer function is used as an extrapolator (but not far from interpolator);
- pixels outside the two convex-hulls: this means that for these pixels, the transfer function will behave as an extrapolator which makes the results less reliable. However, having a priori information on the site may help to evaluate the extrapolation capacities of the transfer function.

Convex-Hull test for sampling strategy : Jarvselja 2005

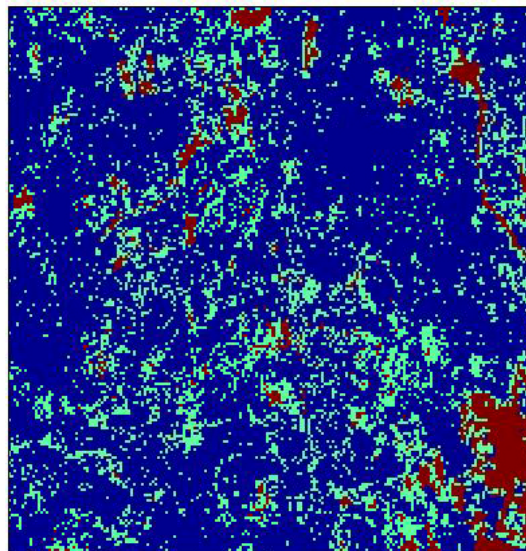


Figure 8. Evaluation of the sampling based on the convex hulls. The map is shown at the bottom: blue and light blue correspond to the pixels belonging to the 'strict' and 'large' convex hulls and red to the pixels for which the transfer function is extrapolating.

The flag map shows that the representativeness of the ESUs is very good, even if pixels are outside the two convex-hulls (mainly in the south-east of the area). They mainly correspond to low NDVI values: open areas, paths, recent clear cuts...

3. Determination of the transfer function for the two biophysical variables: LAI, fCover

3.1. The transfer function considered

Two types of transfer functions are usually tested in the frame of the VALERI project:

- AVE: if the number of ESUs belonging to the class is too low. The transfer function consists only in attributing the average value of the biophysical variable measured on the class to each pixel of the SPOT image belonging to the class;
- REG: if the number of ESUs is sufficient, multiple robust regression between ESUs reflectance (or Simple Ratio) and the considered biophysical variable can be applied: we used the 'robustfit' function from the Matlab statistics toolbox. It uses an iteratively re-weighted least squares algorithm, with the weights at each iteration computed by applying the bisquare function to the residuals from the previous iteration. This algorithm provides lower weight to ESUs that do not fit well. The results are less sensitive to outliers in the



data as compared with ordinary least squares regression. At the end of the processing, three errors are computed: classical root mean square error (RMSE), weighted RMSE (using the weights attributed to each ESU) and cross-validation RMSE (leave-one-out method).

For all the classes, the 'REG' function is tested using either the reflectance or the logarithm of the reflectance for any band combination as well as the simple ratio or NDVI. As the method has poor extrapolation capacities, a flag image, based on the convex hulls is computing over reflectances.

3.2. Results

3.2.1. Choice of the method

For all the ESUs, a single transfer function is computed. Figure 9 shows the results obtained for all the possible band combinations using either the reflectance (ρ) or the logarithm of the reflectance ($\log(\rho)$): even if the regression made on the $\log(\rho)$ provides slightly better results (LAI variable), the results using the reflectance were selected for LAI and fCover. The transfer function using the $\log(\rho)$ indeed creates coplanar points which do not allow the determination of the 'strict' and 'large' convex hulls. The Red*NIR ('+' or RN) combination is added to all the band combinations (except NDVI and SR). Please read the document (http://www.avignon.inra.fr/valeri/table_methods/new_linear.pdf): "A method to improve the relation between the biophysical variables".

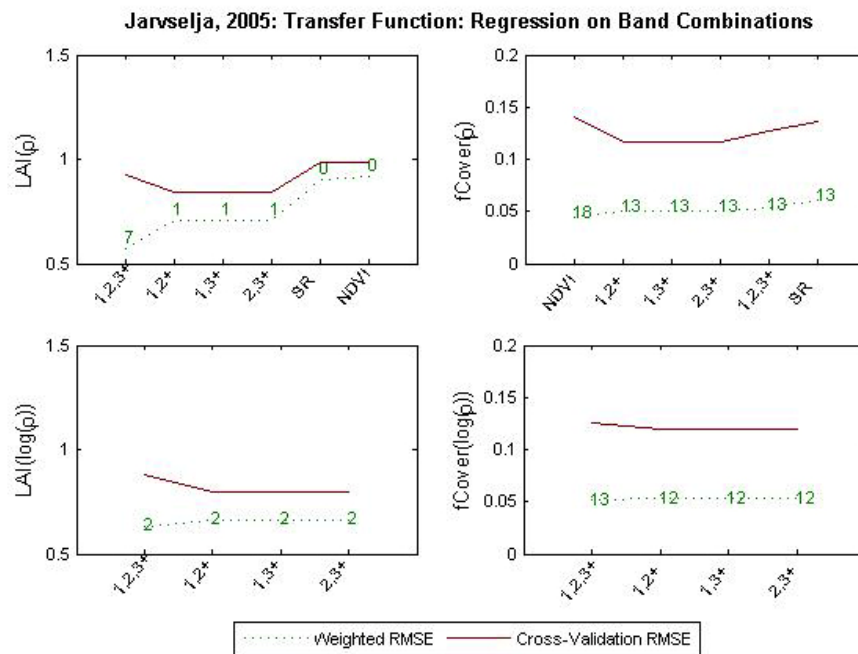


Figure 9. Transfer function: test of multiple regression applied on different band combinations. Band combinations are given in abscissa. The estimated biophysical variable is given in ordinate. Top graphs correspond to regression made on reflectance (ρ): the weighted root mean square error (RMSE) is presented in green along with the cross-validation RMSE in red. The numbers indicate the number of data used for the robust regression with a weight lower than 0.7 that could be considered as outliers. Bottom graphs correspond to regression made on the logarithm of the reflectance.

3.2.2. Choice of the band combination

For the LAI_{eff}, the XS2, XS3, RN combination on reflectance (Figure 10 and Figure 11) was selected since it provides a good compromise between the cross-validation RMSE (lowest value), the weighted RMSE and the RMSE (lowest value). Note that one weight is lower than 0.7. The following band combinations provide the same results: [XS1,XS2,RN] and [XS1,XS3,RN]. Note that the results are close between REG on ρ and REG on $\log(\rho)$.

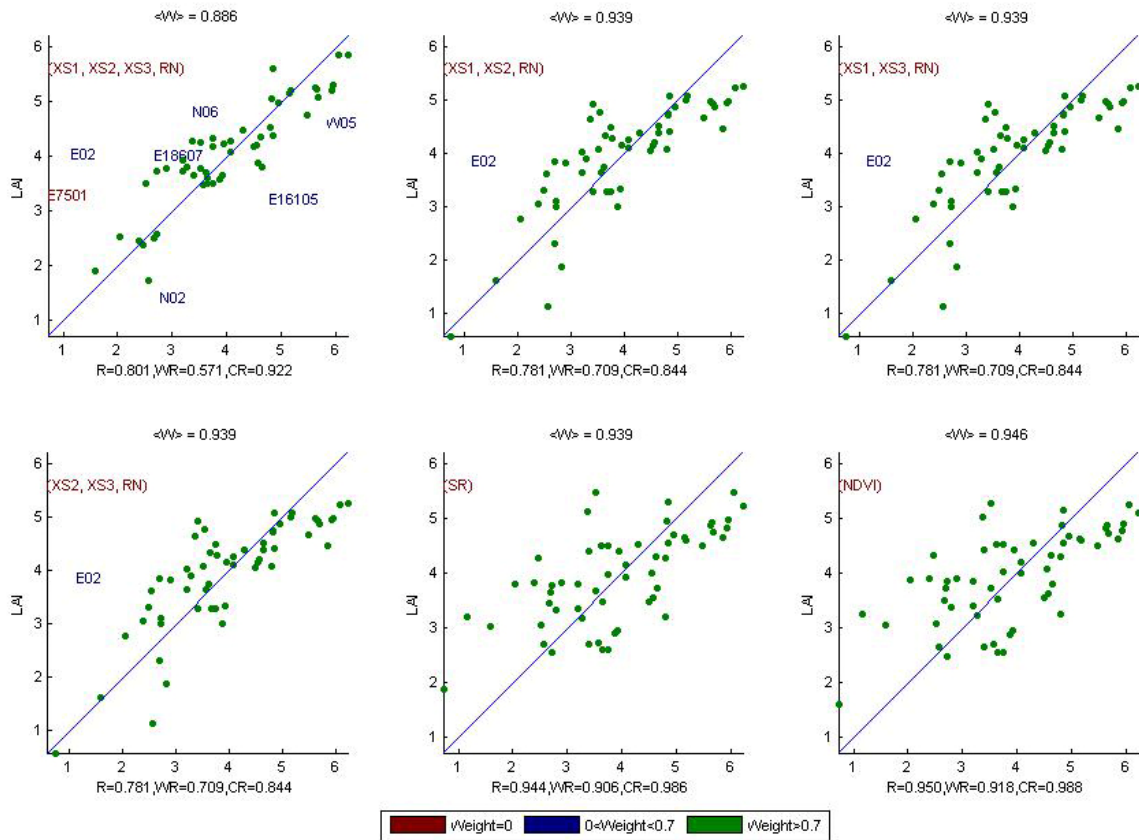


Figure 10. Leaf Area Index: results for regression on reflectance using different band combinations. R is the root mean square error computed between LAI and estimated LAI. WR is the weighted root mean square error and CR is the cross validation root mean square error.

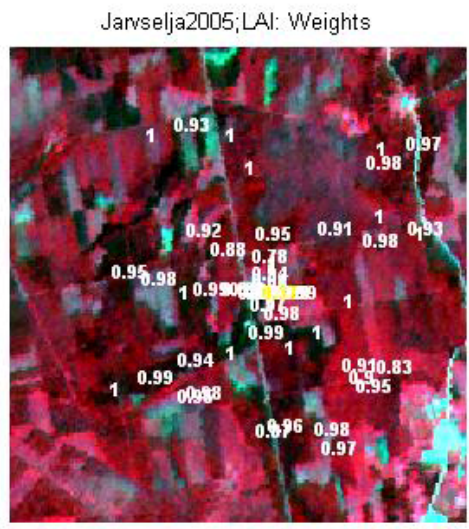


Figure 11. Weights associated to each ESU for the determination of LAI transfer function.

For the fCover, the XS2, XS3, RN combination on reflectance (Figure 12 and Figure 13) was selected since it provides the better results. Note that thirteen weights are lower than 0.7. However, 44 data are used for the robust regression with a weight higher than 0.7. The following band combinations provide the same results: [XS1,XS2,RN] and [XS1,XS3,RN].



Following, the results of the transfer function (Table 2):

Variable	Band Combination	RMSE	Weighted RMSE	Cross-valid RMSE
LAI	$15.299 - 107.2619(XS2) - 136.3691(XS3) + 231.5518(RN)$	0.781	0.709	0.844
fCover	$2.0069 - 8.8634(XS2) - 15.0859(XS3) + 16.3615(RN)$	0.109	0.051	0.116

RN = Red*NIR

Table 2. Transfer function applied to the whole site for LAI and fCover and corresponding errors

3.3. Applying the transfer function to the Järvselja SPOT image extraction

Figure 14 presents the biophysical variable maps obtained with the transfer function described in Table 2 for all the classes. The maps obtained for the two variables are consistent, showing similar patterns: low LAI values where low fCover are observed and conversely...

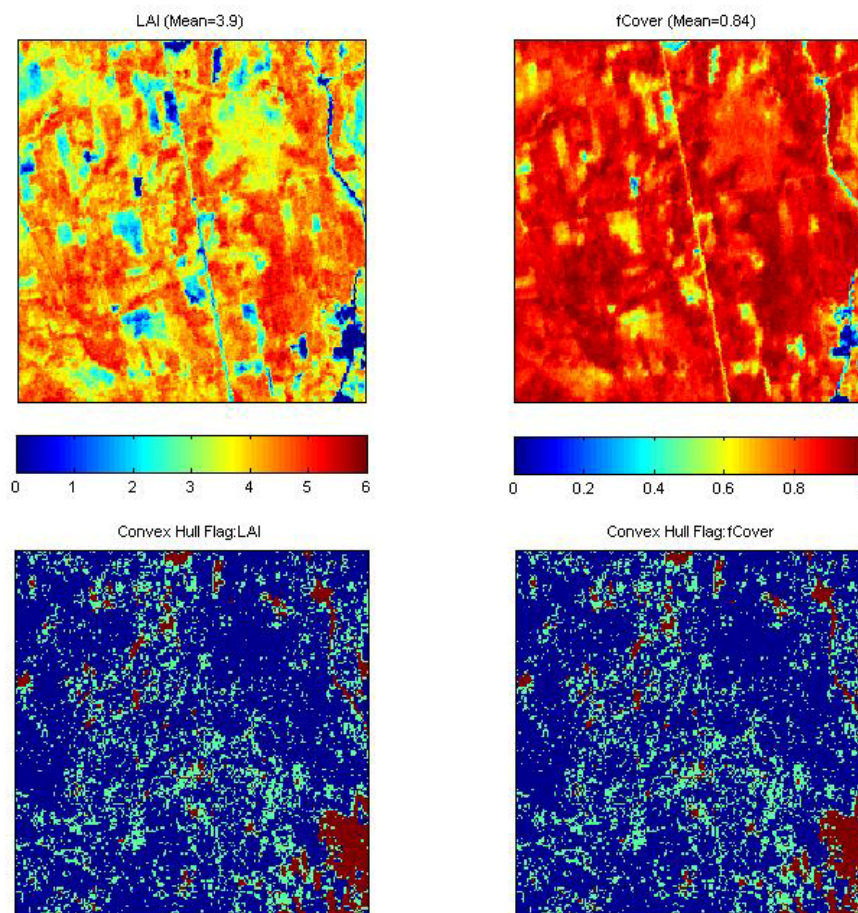


Figure 14. High resolution biophysical variable maps applied on the Järvselja site (top). Associated Flags are shown at the bottom: blue and light blue correspond to the pixels belonging to the ‘strict’ and ‘large’ convex hulls and red to the pixels for which the transfer function is extrapolating

The flag maps are comparable between the two biophysical variables. Note that the pixels outside the two convex-hulls mainly correspond to lowest NDVI values (§2.3.4).

4. Conclusion

The Järvselja site is heterogeneous in terms of LAI and NDVI. The relationship between these two variables is consistent. The representativeness of the land cover of the different ESUs is very good. The ‘REG’ method



(§3.1) is applied to all the classes. The results of the robust regression are good and the maps obtained for the biophysical variables are consistent, even if 23 per cent of the data used for the robust regression applied to fCover could be considered as outliers (§3.2.2). The flag associated to each map shows that the extrapolation of the transfer function is mainly bounded to low NDVI values (open areas, clear cuts...). For LAI and fCover, the regression coefficients are computed by relating the variable itself to reflectance.

The biophysical variable maps are available in Lambert-Est-92 (datum: WGS-84) projection coordinates at 20m resolution.

5. Acknowledgements

We want to thank: **Mait Lang**, **Tõnu Lükk**, **Tiit Nilson** (Tartu Observatory), **Ave Kodar** (Tartu University) and **Alo Eenmäe** (Estonian University of Life Sciences) for the organisation and participation to the campaign.



ANNEX



Ground measurement acquisition report for the VALERI site **Järvelja**

sampled from 28/06/2005 to 01/07/2005

Organization: Tartu Observatory
email: nilson@aai.ee

Date of report: 20.01.2007

People participating to the field experiment:

Firstname & Name	Organization
Tiit Nilson	Tartu Observatory
Mait Lang	Tartu Observatory
Tõnu Lükk	Tartu Observatory
Alo Eenmäe	Estonian University of Life Sciences
Ave Kodar	Tartu University



Site coordinates

	Lat-Long WGS-84 (Deg min.00)		UTM / WGS84 UTM		Other projection* Lambert-Est 1992	
	Lat.	Long.	Easting	Northing	Easting	Northing
Upper left corner	27 14.28408	58 18.76428	513949	6463554	689721	6468147
Lower right corner	27 17.20086	58 17.07156	516811	6460423	692721	6465147

*The other projection user is Lambert-Est 1992. All the characteristics are provided in the following table (see <http://www.avignon.inra.fr/valeri/>, methodology page, GPS document for more information):

Geodesic Map Datum		Map Projection	
Associated Ellipsoid	WGS-84	Latitude of origin	57.51755393055N
Semi-major axe	6 378 137	Longitude of origin	24.00 E
Semi-minor axe	6 356 752.3	Parallels:	
1/flattening	298.257 223 563	1 st	58.00 N
		2 nd	59.333333 N
Eccentricity	0.081819190842622	Xo: false easting	500000
		Yo: false northing	6375000
		Scale factor	1

Ground control points

Control points were located from 1:50000 digital map of Estonia. Co-ordinate system used: Lambert-Est 1992.

Description of the site and land cover

Comments on the land cover

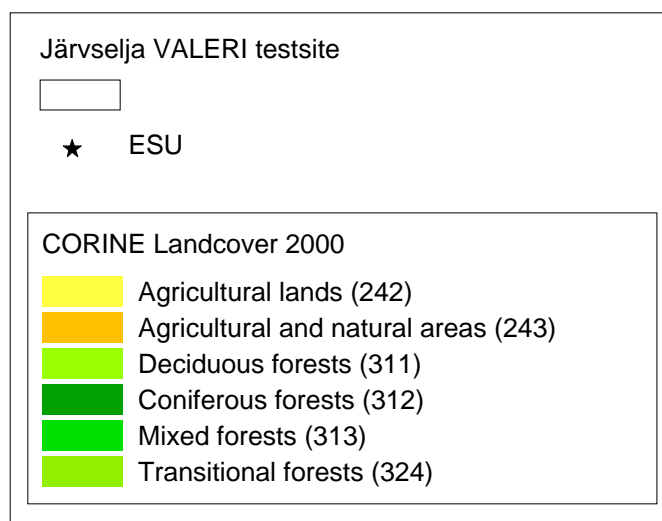
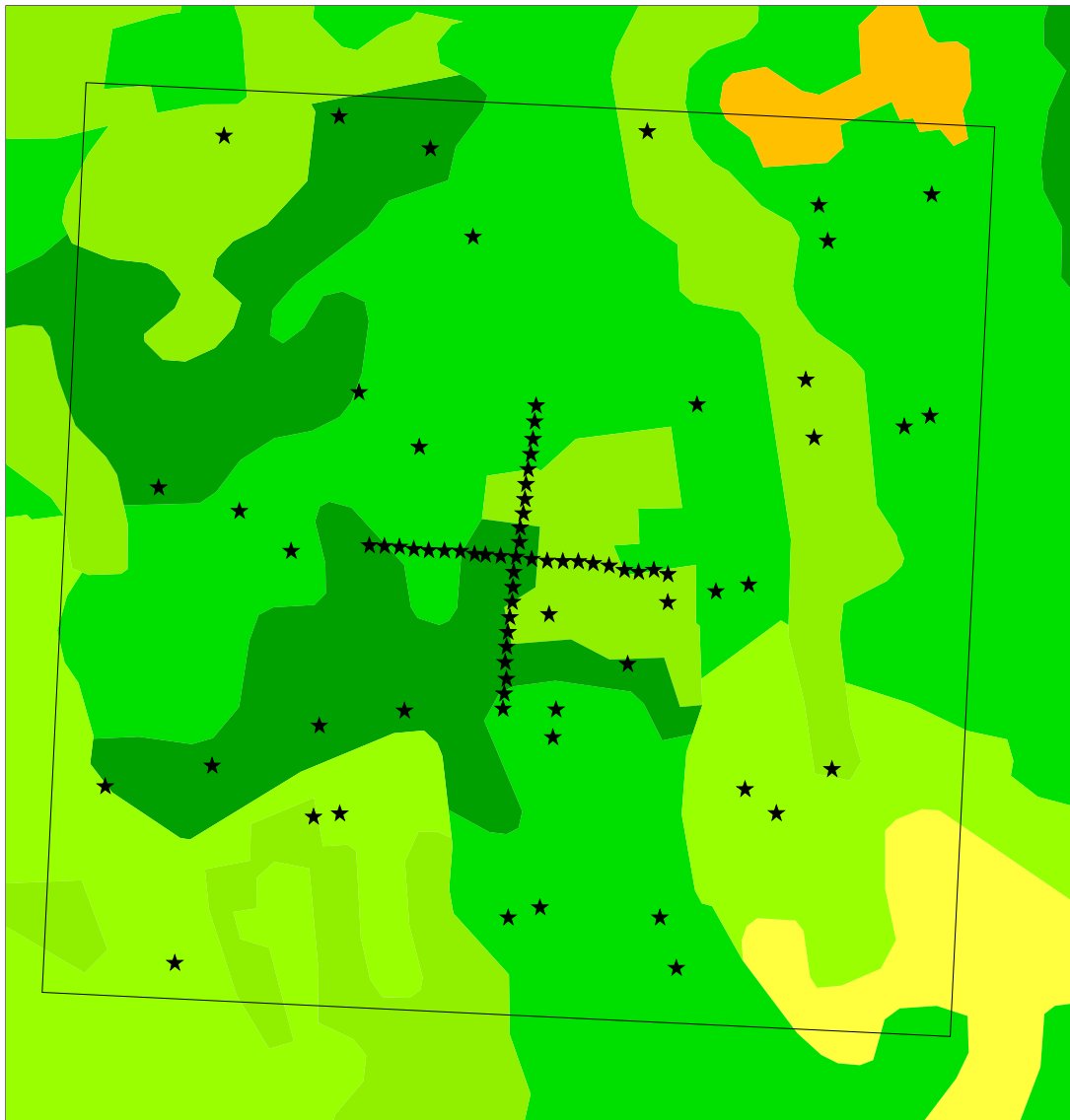
Boreal forests.

Topography

Flat.



Land cover map



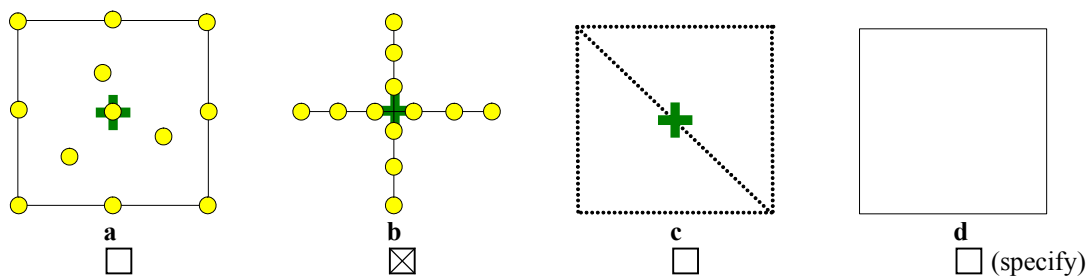


Spatial Sampling scheme

Sensors used for sampling the ESUs

	Method	Comments
<input checked="" type="checkbox"/>	Hemispherical photographs	
<input checked="" type="checkbox"/>	LAI2000	
<input type="checkbox"/>	TRAC	
<input type="checkbox"/>	Ceptometer	
<input type="checkbox"/>	Direct measurements	
<input type="checkbox"/>	Other	

Sampling strategy for the ESU



Distribution of the Elementary sampling units

The high spatial resolution image

Satellite

Satellite used: SPOT2 HRV1
 Level of processing: 1B
 Projection type: Lambert-Est 1992
 Acquisition date:
 Georeferencing comment (accuracy, waypoint validation ...): residual error 4.6 m.



List of the ESUs

Plot #	Easting(m)	Northing(m)	Vegetation
X00	691213	6466658	Spruce understorey, 2m. Thinning 1994, 1997.
E01	691265	6466653	
E02	691316	6466650	2nd storey spruce, h=13m. Thinning 1994, 1997. Thinning 2005
E03	691368	6466651	clearcut.
E04	691419	6466653	Thinning 1995.
E05	691468	6466649	Thinning 1995.
W01	691162	6466658	
W02	691112	6466660	Thinning 1994, 1995.
W03	691076	6466661	Spruce understorey 4m. Thinning 2003
W04	691028	6466668	Spruce understorey 4m. Thinning 2003
W05	690976	6466667	Spruce understorey 4m. Thinning 2003
N01	691222	6466707	Spruce understorey, 2m. Thinning 1994, 1997.
N02	691222	6466755	Spruce understorey, 1m. Sanitary thinning 1996, 1997.
N03	691230	6466802	Spruce understorey, 1m. Sanitary thinning 1996, 1997.
N04	691233	6466849	Recent clear cut. Clear cut 1997.
N05	691234	6466899	2nd storey spruce and birch, h=8m. Sanitary thinning 1997. Thinning 2004
N06	691239	6466948	2nd storey spruce and birch, h=8m. Sanitary thinning 1997. Thinning 2004
16503	691598	6466323	Sanitary thinning 1996.
13904	691877	6466576	2nd storey spruce, h=12m.
13902	691984	6466040	2nd storey spruce, h=12m.
15905	689896	6465837	2nd storey spruce, h=8m.
16004	690245	6465922	2nd storey spruce, h=14m. Sanitary thinnings 1995, 1997.
16105	690592	6466071	2nd storey spruce, 21m. Sanitary thinning, 1996, 1997.
16111	690673	6465785	Spruce understorey, 4m.
16110	690587	6465770	Clear cut in 2001.
16206	690870	6466134	2nd storey spruce, h=10m.
7302	690184	6467996	
7403	690560	6468079	2nd storey spruce, h=13m. Thinnings 1995, 1997.
7501	690865	6467988	2nd storey spruce 14m. Sanitary thinning 1995, 1996, 1997. Clearcut 2005 spring
7604	691020	6467704	
10417	690024	6466829	
13401	690294	6466764	
13403	690471	6466641	Birch regeneration on previous clear cut. 2003 June birches cut and lay on the ground in July.
10608	690669	6467174	Clear cut. Clear cut.
10712	690877	6467004	Sanitary thinning 1995.
16713	692288	6466010	Regenerating clear cut.
18902	692112	6465856	
16605	692005	6465930	
18608	691348	6465508	Thinned 1999.
18607	691245	6465470	2nd storey spruce, h=7m. Heavy thinning 2001.
18806	691745	6465494	2nd storey spruce, h=12m. Sanitary thinning 1997.
18809	691807	6465331	2nd storey spruce, h=2m. Thinned in 2003.
16404	691369	6466162	Spruce understorey 8m. Sanitary thinning 1995.
13708	691331	6466474	Clear cut. Clear cut 1997.
S01	691208	6466608	Spruce understorey, 2m. Thinning 1994, 1997.
S02	691208	6466558	Spruce understorey, 2m. Thinning 1994, 1997.
S07	691194	6466309	Spruce understorey, 4m. Sanitary thinning 1996.
11004	691785	6467188	
11117	692139	6467287	
14003	692176	6467098	
14104	692554	6467188	2nd storey spruce.
14102	692471	6467149	
32816	692524	6467917	
11104	692189	6467747	
7914	692154	6467864	
N10	691255	6467159	2nd storey spruce, h=5m.
W10	690728	6466672	2nd storey spruce 8m. Thinning 2003